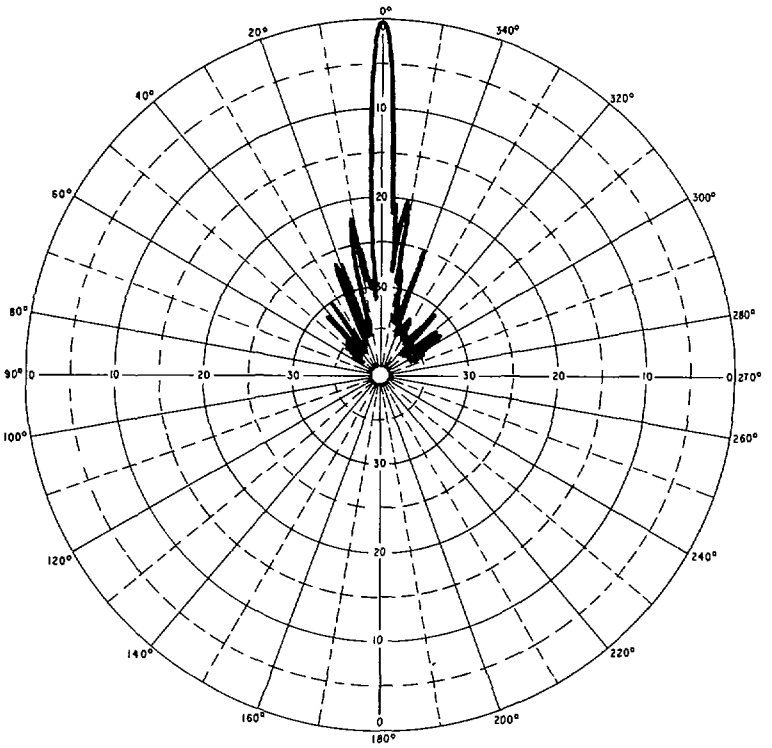

Fig. 6. *H*-plane radiation pattern (38.4 GHz).

array indicate that mismatches within the microstrip feed network are responsible for the degraded sidelobe and gain performance. Possible sources of these mismatches are substrate and etching nonuniformity.

SUMMARY AND CONCLUSION

The results of this study are very encouraging and show the feasibility of the microstrip antenna approach at millimeter wave frequencies. All results presented were from actual measurements performed on full scale models at 36.6, 38.4, and 57.4 GHz.

Microstrip Series Arrays

THOMAS METZLER

Abstract—**A traveling-wave design technique for microstrip series arrays is discussed. The technique is applicable to both resonant and nonresonant array configurations. Experimental results for both configurations are presented.**

I. INTRODUCTION

Series array configurations offer unique advantages to the microstrip antenna designer. First, feed line lengths are inherently minimized, thus reducing line radiation and dissipation losses which decrease array efficiency. Further, in large arrays high-power feed lines are decoupled from elements radiating low-power levels. This permits tighter control of aperture distributions. Finally, steered beams can be easily achieved, and the series configuration is particularly applicable when frequency scanning is desired.

In recent years several theoretical models for microstrip series arrays have been developed which are based on either waveguide [1] or resonant cavity analogies to the microstrip circuit. However, when these models are applied to practical designs, anomalies are observed in the measured patterns such as increased sidelobes and unpredictable beam positions. This communication discusses the problems encountered in designing microstrip series arrays, and presents an empirical design approach which circumvents certain problems that are not easily solved analytically.

II. DESIGN APPROACH

The microstrip element is typically modeled as two radiating slots formed by patch edge discontinuities interconnected by a low-impedance microstrip line [2]. The radiation conductance is calculated from the equivalent slot width, and the susceptance is the computed open-circuit capacitance of the low-impedance line.

Our initial work attempted to model the series array as cascaded elements interconnected by high-impedance lines. In theory all critical parameters (phase velocity and slot conductance) could be calculated and the array designed analytically. This approach was reasonably successful for arrays consisting of a small number of elements; however, some anomalies such as moderate beam squint and increased sidelobes were observed. Extending these methods to large

Manuscript received February 29, 1980; revised July 25, 1980.

The author is with Ball Aerospace Systems Division, Boulder, CO 80303.

0018-926X/81/0100-0174$00.75

arrays proved unsuccessful, and it was noted that an unpredicted phase shift was measured across the array. This effect was observed by both near-field probing and measured far-field patterns of resonant arrays which exhibited squint instead of broadside beams.

Our approach was to treat the array as a traveling-wave structure, and empirical design curves were developed. Nonresonant test arrays consisting of 26 similar resonant elements were fabricated on a 0.250-in honeycomb substrate. The insertion loss and beam squint angle of each array was measured. Based on these data, design curves relating phase velocity and radiation conductance to the element width were formulated and are discussed below.

The measured array insertion loss can be related to the normalized radiation conductance of the element by the following formula [3]:

$$10 \log (1 + g) = \frac{\text{insertion loss in decibels}}{N}, \tag{1}$$

where g is the normalized element conductance (normalized to feed line conductance), N is the number of elements in the array, and insertion loss is the power available at the array input divided by the power transmitted through the array. The array insertion loss consists of both radiation and I^2R losses. However, the dissipated loss can be calculated and the measured insertion loss modified such that it reflects only the radiation loss.

The measured data yielded a design curve given by the following:

$$G = 0.016 \, (W/\lambda_0)^{1.757}, \tag{2}$$

where G is the element radiation conductance in mhos (not normalized) and W is the element width. It has been shown that the theoretical radiation conductance of a resonant microstrip element is given by

$$G = 2/90 \, (W/\lambda_0)^2, \qquad W/\lambda_0 \ll 1 \tag{3}$$

$$G = 2/120 \, (W/\lambda_0), \qquad W/\lambda_0 \gg 1. \tag{4}$$

The experimental values for (W/λ_0) varied from 0.033 to 0.254. The emperically derived equation is in good agreement with the first theoretical equation given above, which is valid for small element widths.

In addition, the phase velocity in each test array was determined from the measured beam pointing angle. In a traveling wave array the beam position is given by

$$\cos \theta = \lambda/\lambda_Z - \lambda/S, \tag{5}$$

where θ is the angle measured from end fire, λ_Z is the wavelength in substrate, and S is the element spacing. By measuring the beam steering angle, λ/λ_Z (which is directly related to the phase velocity) can be calculated. Two important facts were observed from this measurement. First, the phase difference between elements was much larger than could be accounted for by simple line length calculations. This phase difference increased linearly with element width, implying that the junction discontinuities introduced an added phase shift proportional to the discontinuity size. This additional phase shift accounts for the failure of the initial analytic models. Second, the arrays were dispersive. Again, this dispersion was porportional to the discontinuity size. With the arrays composed of smaller width elements, no dispersion over the frequency band of interest was observed. The functional relationship between phase velocity and element width was determined and used to calculate the required element "resonant" width and spacings for a given beam angle.

III. RESONANT ARRAY TEST RESULTS

In a resonant array the radiating elements are spaced by 1 λ in the dielectric and radiate in-phase, forming a broadside beam. The array may be the center-fed if a 180° phase difference is introduced between the array halves to compensate for their spatial orientation. The input admittance of each array section is simply the sum of the element admittances, and the power radiated by each element is equal to the ratio of the element admittance to the array input admittance. Since the phase velocity differs for elements of different width, a nonuniform distribution of element spacing is required to maintain the correct phase distribution.

The resonant array is highly efficient. The length of the transmission line connecting each element is inherently minimized by the series configuration. Also, in a center-fed array a significant portion of the input power is radiated in the first few elements and does not suffer from extensive line length loss.

A 5-m resonant array consisting of 26 elements was fabricated on a 0.25-in Nomex honeycomb. The ground plane and antenna circuit were 0.005-in copper-clad G-10 laminated to the honeycomb. The element nonresonant width varied from 0.32 λ to 0.10 λ, with an element spacing of 1 λ in the dielectric. The array was designed for 30-dB sidelobes using a Taylor distribution. Integration of the ideal pattern yielded a theoretical directivity of 22.2 dB.

A measured antenna pattern and voltage standing-wave ratio (VSWR) plot are shown in Fig. 1. The sidelobes were generally below 26 dB, with the exception of one at 22 dB which appeared to be a range reflection. The measured gain was 21.2 dB, with a mismatch loss of 0.3 dB (1.8:1 VSWR) at 1.420 GHz. The antenna gain is 0.7 dB lower than the theoretical directivity, yielding an array efficiency of 85 percent. If a standard microstrip corporate feed had been used, feed line dissipative losses would have been almost 1.4 dB. Thus in this configuration the series array is almost twice as efficient as a standard microstrip array.

The resonant array is bandwidth-limited in terms of both impedance and pattern performance. The sidelobe levels quickly approach 22 dB at 1.400 and 1.430 GHz.

IV. NONRESONANT ARRAY TEST RESULTS

In a traveling-wave array the element spacing is other than 1 λ, and a linear phase taper exists across the array. The beam is thus scanned off broadside with the scan angle a function of frequency. As in the resonant array, amplitude tapers are implemented by varying the nonresonant patch dimensions.

Fig. 2 illustrates a typical radiation pattern and impedance locus of the 5-m traveling-wave array. An inverted microstrip configuration was utilized in the array construction to reduce dielectric losses. The array consisted of 28 elements with the element widths varying from 0.23 λ to 0.08 λ. The element spacing was 0.89 dielectric wavelengths.

The measured array gain was 21.5 dB with 0.2 dB of the

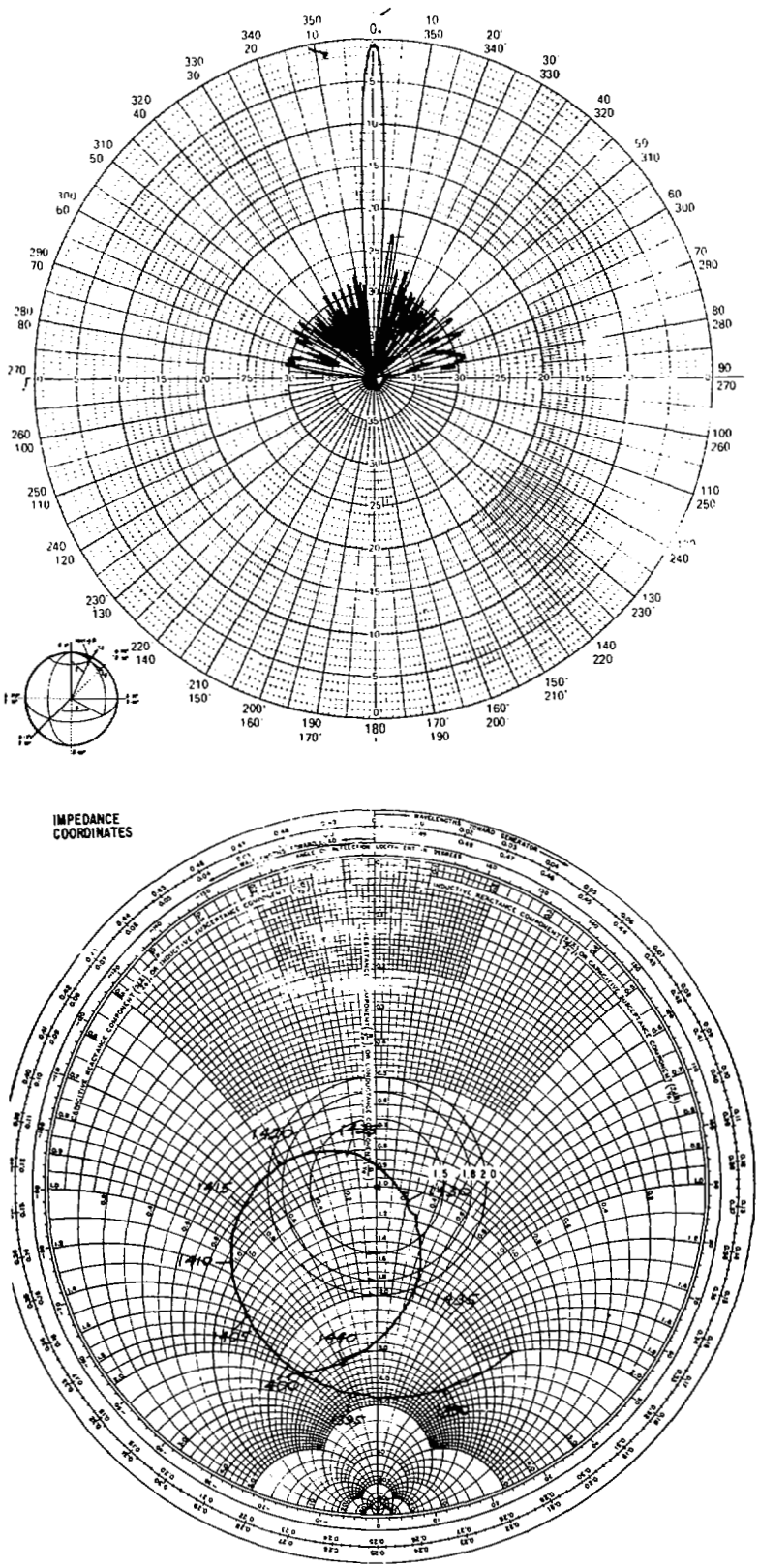

Fig. 1. Measured pattern and impedance performance of 5-m resonant series array.

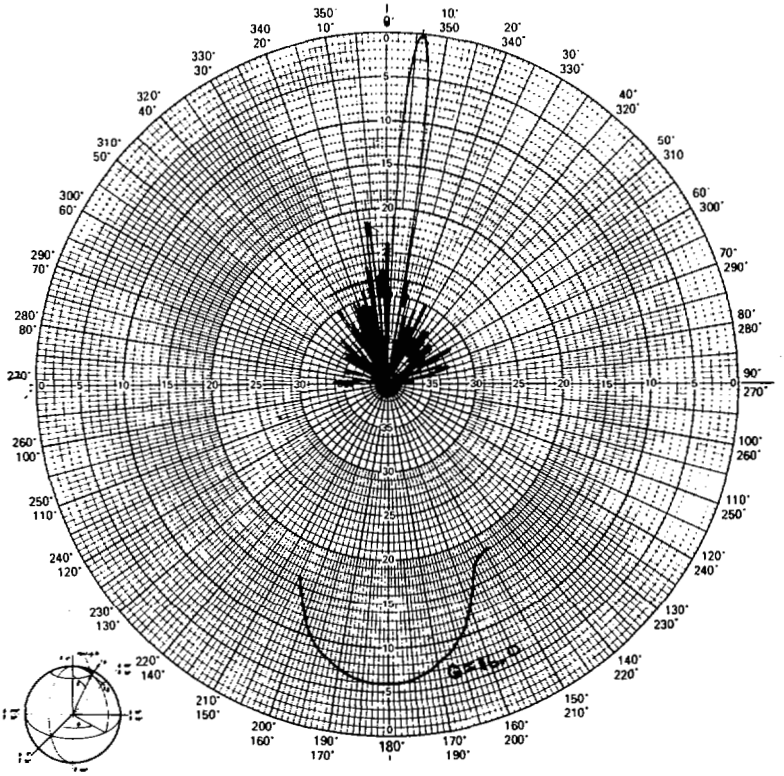

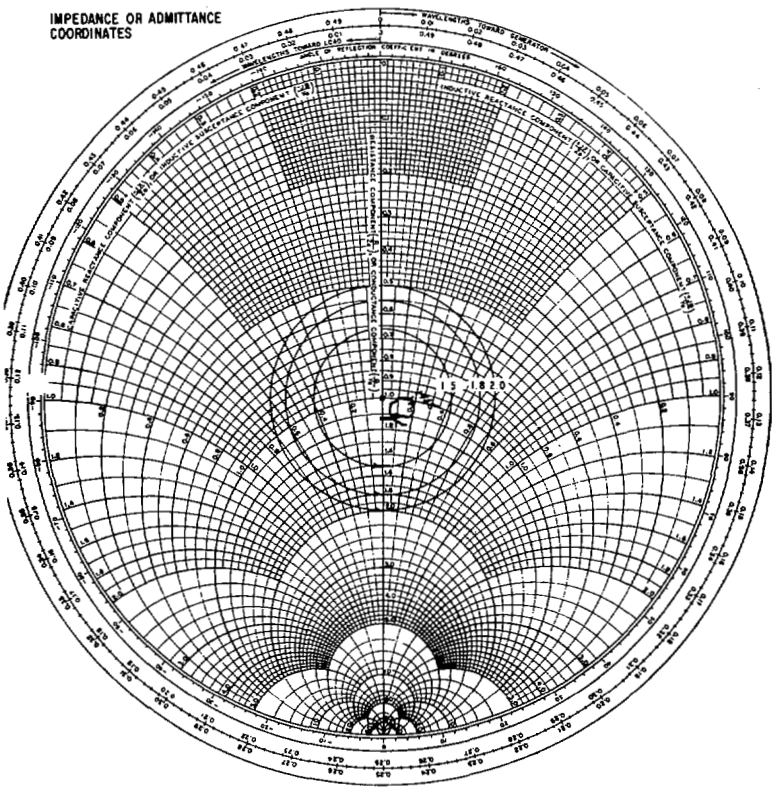

Fig. 2. Measured pattern and impedance performance of 5-m traveling wave array.

input power dissipated in a terminating load. The theoretical directivity is 22.2 dB. The gain and pattern performance was maintained over a six-percent bandwidth. With the exception of an image beam, sidelobes remained below 23 dB over this bandwidth. From 1400 GHz to 1430 the array scanned 2°.

V. CONCLUSION

Microstrip series arrays are efficient radiators, and in the traveling wave configuration performance is maintained over a relatively large bandwidth. These arrays represent a monolithic printed-circuit design that may find application not only when high efficiency is required but also in frequency-scanned applications.

REFERENCES

[1] A. Derneryd, "Linearly polarized microstrip antennas," *IEEE Trans. Antennas Propagat.*, vol. AP-24, pp. 846–850, Nov. 1976.
[2] R. E. Munson, "Conformal microstrip antennas and microstrip phased arrays," *IEEE Trans. Antennas Propagat.*, vol. AP-22, pp. 74–78, Jan. 1974.
[3] H. Jasik, Ed., *Antenna Engineering Handbook*, 1st ed. New York: McGraw Hill, 1961, ch. 16, pp. 28–32.

An Extremely Lightweight Fuselage-Integrated Phased Array for Airborne Applications

JAMES S. YEE, SENIOR MEMBER, IEEE, AND
WILLIAM J. FURLONG

***Abstract*—A design of a lightweight low volume electronically scanned antenna is described. This antenna, besides being the radiating aperture, serves as a load-sharing fuselage panel in a small weight-sensitive remotely piloted vehicle (RPV). A demonstration array incorporating the microstrip radiating elements, stripline feed circuit, and microstrip-line p-i-n diode phase shifters was assembled to evaluate the electrical characteristics and scanning capabilities of the array. The demonstration array was tested on the antenna range and operated successfully as part of a radar/communication subsystem demonstration. An eight-element lightweight section of the demonstration array was subsequently designed and fabricated in a modern production facility utilizing numerically controlled machines and state-of-the-art printed circuit board etching and plating equipment. Successful operation of this lightweight section sufficiently demonstrated that a lightweight and low volume electronically steerable phase-array antenna can be fabricated and integrated into a structural panel in production quantities.**

I. INTRODUCTION

Lightweight, low volume, low cost, and high performance are familiar requirements for airborne antenna systems. Technological advances in lightweight low volume radiating element designs and advances in lightweight high-density packaging techniques for RF components and devices in microstrips and striplines make airborne phased-array designs possible. The unique feature of this design is the application and integration of these technologies to achieve an antenna/fuselage panel which serves as the antenna aperture and load-sharing structure in a small weight-sensitive remotely piloted vechicle (RPV). This communication discusses the critical electrical and mechanical design concepts necessary to achieve the desired weight and performance characteristics.

Manuscript received February 1, 1980; revised August 30, 1980.
The authors are with the Boeing Military Airplane Company, Advanced Airplane Branch, P. O. Box 3707, Seattle, WA 98124.

II. RADIATING ELEMENT DESIGN

The microstrip radiating element design was based on the work of John Q. Howell [1]. The element is a conducting disk supported by a thin layer of low-loss dielectric substrate which rests on a conducting ground plane. The essential parts of the element are shown in Fig. 1(a). Also shown is the element *E*-plane radiation pattern. The disk diameter for resonance is primarily determined by the dielectric constant of the substrate material beneath the disk and the resonance mode that is excited inside the disk. Howell based the resonant diameter determination on the TM_{11} mode of a circular resonant structure in a microstrip [2]. Generally, this initial determination is a good starting point, but the exact diameter for resonance requires additional fine trimming in the laboratory. It was found that the diameter for resonance is also a function of probe offset, substrate thickness, and the disk physical environment, such as the substrate material extending beyond the top conducting disk and the size of the ground plane. The patterns shown in Fig. 1 were recorded with the microstrip element on a 16 × 16 in ground plane. The term "resonance" used in this paper is referring to that frequency which crosses the zero-reactance line in the swept frequency-impedance plot on the Smith chart.

The feed point offset distance from the disk center determines primarily the impedance match at resonance. Since the disk is ordinarily fed with a 50 Ω line, Howell [1] suggested an initial offset distance of approximately one-third of the radius from the center for a substrate material whose dielectric constant is 2.6. Final offset distance trimming is required to achieve good impedance match. Since the trend of behavior on resonance and on impedance match due to the above two dimensions is generally predictable, a little laboratory experimentation will provide a workable design fairly rapidly.

A very desirable feature of this radiating element design is the ease of obtaining radiation in the orthogonal polarization. This can be accomplished by locating the feed point at the same offset position 90° away from the original feed point. Circular polarization radiation is easily obtained by exciting the two orthogonal feed points of the same offset simultaneously with a 90° 3-dB hybrid. A typical spinning linearly polarized radiation pattern for an element excited to give circular polarization is shown in Fig. 1(b). The pattern performance quality (axial ratio) is determined by the excursion of the pattern trace. Since the excursion is less than 1 dB over a wide angular portion of the pattern, the radiation pattern is considered nearly circularly polarized.

III. DEMONSTRATION ARRAY

Prior to any detailed production and packaging design considerations, it was deemed necessary to design an array using the circular disk microstrip elements described in Section II and to design the stripline feed components and p-i-n diode

0018-926X/81/0100-0178$00.75